Journal of Power Sources 195 (2010) 5929–5933

Contents lists available at ScienceDirect

Journal of Power Sources

journal homepage: www.elsevier.com/locate/jpowsour

Short communication

Morphological features of electrodeposited Pt nanoparticles and its application as anode catalysts in polymer electrolyte formic acid fuel cells

Hongrae Jeon [a], Jiyong Joo [a], Youngkook Kwon [a], Sunghyun Uhm [b], Jaeyoung Lee [a,b,*]

[a] Electrochemical Reaction & Technology Laboratory (ERTL), Department of Environmental Science and Engineering, GIST, Gwangju 500-712, South Korea
[b] Ertl Center for Electrochemistry and Catalysis, GIST, Gwangju 500-712, South Korea

ARTICLE INFO

Article history:
Received 28 October 2009
Received in revised form 9 January 2010
Accepted 4 March 2010
Available online 10 March 2010

Keywords:
Platinum
Anode catalysts
Electrodeposition
Formic acid oxidation
Fuel cells

ABSTRACT

Electrodeposited Pt nanoparticles on carbon substrate show various morphologies depending on the applied potentials. Dendritic, pyramidal, cauliflower-like, and hemi-spherical morphologies of Pt are formed at potential ranges between −0.2 and 0.3 V (vs. Ag/AgCl) and its particle sizes are distributed from 8 to 26 nm. Dendritic bulky particles over 20 nm are formed at an applied potential of −0.2 V, while low deposition potential of 0.2 V causes dense hemi-spherical structure of Pt less than 10 nm. The influence of different Pt shapes on an electrocatalytic oxidation of formic acid is represented. Consequently, homogeneous distribution of Pt nanoparticles with average particle of ca. 14 nm on carbon paper results in a high surface to volume ratio and the better power performance in a fuel cell application.

1. Introduction

Direct formic acid fuel cells (DFAFCs) have been emerged since early 2000s due to the high energy density, fast oxidation kinetics, and safety of liquid formic acid (HCOOH), as well as simple integration in a portable power device [1–3]. Among various catalysts Pt is still a well-known anode catalyst for the electrooxidation of formic acid in spite of the problem of being strongly poisoned by intermediate species [4–6].

To date, great efforts have been made to increase the ratio of surface area to volume of Pt nanoparticles by reducing the size because a rough surface containing terraced, stepped, and kinked sites is generally more active than a flat, low-index surface [7]. In addition, a number of chemical routes also have been developed to produce Pt nanostructures such as spheres, cubes, rods, wires, prisms, and multipods [8–12], since the catalytic and electrocatalytic activity depend on not only the ratio of surface area to volume, but also the structure or arrangement of atoms on the surface [7].

One method to prepare Pt nanostructures, electrochemical deposition reducing metal ions onto selected electrodes is a promising technique due to its easy-to-use procedure and low cost of implementation [13]. However, a large number of electrodeposition conditions including precursor concentration, additives, current density, temperature, agitation, and polarization should be considered [14]. For instance, Tian et al. [13] regulated the shape of the nanoparticles with different electrodeposition current densities and flower-like Pt nanoparticles showed 1.9 times higher catalytic activity than bare Pt on electro-oxidation of methanol. Jayashree et al. [15] observed smooth and dendritic morphologies with different electrodeposition potentials of −1 and −2 V (vs. Ag/AgCl), respectively and dendritic structures with high surface area exhibited increased activity for formic acid oxidation. In addition, we have recently demonstrated that irreversible modification of the Pt metal surface to enhance the performance as well as the durability of the catalyst by underpotential deposition (UPD) with foreign metal adatoms such as Bi [3,6], Pb [16], and Sb [17] is a powerful method to drive a practical DFAFC system.

In this study, we electrodeposited various morphologies of Pt nanoparticles on carbon paper by applying different overpotentials and each structure represented diverse catalytic activities for formic acid oxidation. The dominant effect on DFAFC performance between Pt morphology and particle size is discussed.

2. Experimental

Carbon paper (TGPH-060, E-TEK) was prepared as a catalyst support; electrochemically oxidized at a constant potential of 2.0 V

* Corresponding author at: Electrochemical Reaction & Technology Laboratory (ERTL), DESE, GIST, Gwangju 500-712, South Korea. Tel.: +82 62 970 2440; fax: +82 62 970 2434.
E-mail address: jaeyoung@gist.ac.kr (J. Lee).

0378-7753/$ – see front matter © 2010 Published by Elsevier B.V.
doi:10.1016/j.jpowsour.2010.03.009

in 0.5 M $HClO_4$ for 2 min with a potentiostat/galvanostat (Autolab PGSTAT30) using an Ag/AgCl reference electrode and a platinized Pt counter electrode. After the electrochemical oxidation, Pt was electrodeposited on treated carbon paper in 10 mM H_2PtCl_6 (Sigma), 0.2 mM $Pb(CH_3COO)_2$ (Junsei), and 0.5 M $HClO_4$ (Aldrich). Pb is used as an additive to reduce surface diffusion of Pt atoms which leads to a rough Pt morphology [18]. Prior to the Pt electrodeposition, linear sweep voltammogram (LSV) at 10 mV s^{-1} was conducted to determine the deposition potentials ranging from −0.2 to 0.3 V with the interval of 0.1 V. The amount of deposited metal was controlled by applying the total charge to 1.5 C. Pt/C electrode was prepared by dispersing appropriate amounts of supported catalysts powder (40% mass) in deionized water, 7% Nafion solution (Aldrich), 2-propanol, sonicating the solution for 90 s and catalyst inks were coated on a GDL/carbon paper (TGPH-060, E-TEK). Catalyst loading was adjusted to the same weight of the electrodeposited Pt. To investigate real surface area of electrodeposited Pt, CVs were recorded at 50 mV s^{-1} in 0.5 M $HClO_4$. Structural analysis of Pt was carried out using XRD (D/MAX Ultima III diffractometer). The surface morphologies and electron diffraction (ED) patterns were characterized with a FE-SEM (Hitachi S-4700) and TEM (JEOL JEM-2100), respectively.

In a fuel cell operation [3,19,20], the electrodeposited Pt and commercial Pt/C (0.5 mg cm^{-2}) were used as anode catalysts and commercial Pt black (3.0 mg cm^{-2}, Alfa Aesar) was used as the cathode catalysts. Cathode was prepared by dispersing appropriate amounts of unsupported catalysts powder in deionized water, 5% nafion solution (Aldrich), and 2-propanol, sonicating the solution for 90 s and catalyst inks were coated on a GDL/carbon paper (SGL 35BC). Then, additional ionomer solution was sprayed onto the catalyst layers of anode (0.5 mg cm^{-2}) and cathode (0.15 mg cm^{-2}) in order to decrease the contact resistance with polymer electrolyte membrane (Nafion 115, DuPont). Membrane electrode assemblies (MEAs), with an electrode area of 9 cm^2, were prepared by hot pressing with Nafion 115 at a temperature of 140 °C and a pressure of 100 kg_f cm^{-2} for 5 min. The cell operating temperature was fixed at 60 °C and the concentration of formic acid was 3 M. Air was applied to cathode compartment with the relative humidity of 80% at a flow rate of 200 sccm. Polarization curves and voltage variation with time at constant current were obtained using a fuel cell test station (Scitech Korea).

3. Results and discussion

The electrodeposition of Pt nanoparticles on carbon electrode is characterized by LSV and current profiles at constant potentials in Fig. 1. Cathodic current starts from 0.65 V and several peaks appear below 0.3 V which corresponds to the potentials of $PtCl_6^{2-}$ reduction in Fig. 1(a). Hydrogen adsorption and evolution reactions on as-deposited Pt catalyst caused drastic current drop below −0.2 V. Based on the LSV results, several constant potentials ranging from −0.2 to 0.3 V with the interval of 0.1 V were selected for proper comparison of electrodeposition potentials of Pt as the anode electrocatalyst for formic acid oxidation. The mass loading of Pt is 0.5 mg cm^{-2} and it is enough for DFAFC operation in our previous study [6]. Different electrodeposition time was considered for applying same amount of charges.

The morphologies of the electrodeposited Pt on carbon substrate with different applied potentials are compared. In Fig. 2(a), Pt nanoparticles at a potential of −0.2 V shows bulky dendrite structure that is generally formed under mass transport limited conditions [21]. As applied potential increases, the Pt was homogeneously placed on carbon substrate keeping pyramidal structures between −0.1 and 0 V. Cauliflower-like and hemi-spherical structures were observed at 0.1 and 0.3 V, respectively. In particular, the structure of Pt at 0.3 V is perfectly round with smooth surface and stands apart from each other. Accordingly, high deposition potentials ranging from 0.1 to 0.3 V supplied limited currents for nucleation of Pt which caused isolated and densely agglomerated round structures. On the other hand, sufficient currents of low potentials below 0.0 V induced well-dispersed pyramidal Pt and bulky dendrite structure due to the heterogenous nucleation and limited Pt ion supply in outmost surface of the substrate.

The relationship between the crystallinity and particle size of electrodeposited Pt was analyzed. All three peaks in Fig. 3 correspond to Pt(1 1 1), Pt(2 0 0), and Pt(2 2 0), and Pt(1 1 1) surface was selectively grown on the carbon substrate. Higher crystalline Pt was obtained by applying low potentials and intensity gradually decreased with increasing applied potentials. Although crystallinity of electrodeposited Pt shows potential dependence, its relative intensity of each surface was almost constant. Generally formic acid oxidation on Pt shows structural sensitivity depending on a single crystal surface [22–24]. However electrode-

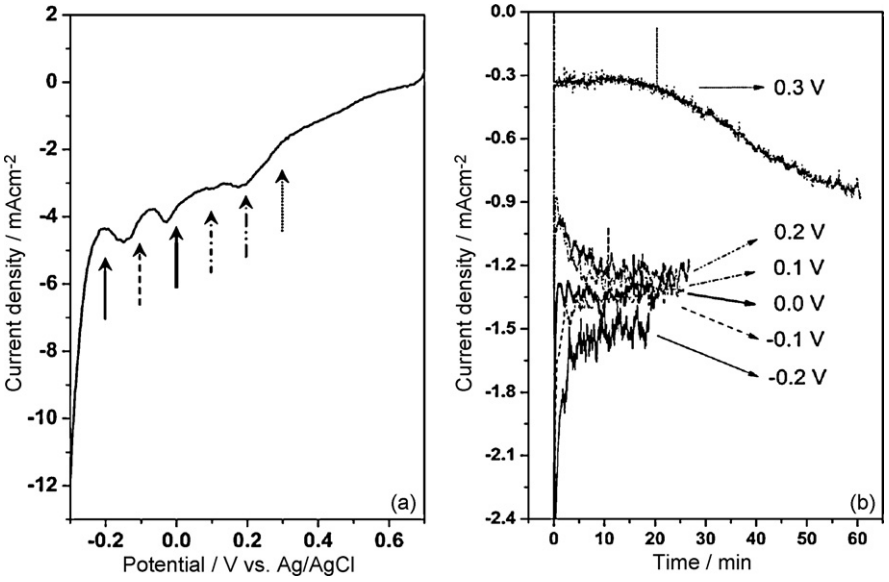

Fig. 1. (a) Linear sweep voltammogram and (b) current versus time profile during potentiostatic deposition in 10 mM H_2PtCl_6 and 0.5 M $HClO_4$ solution.

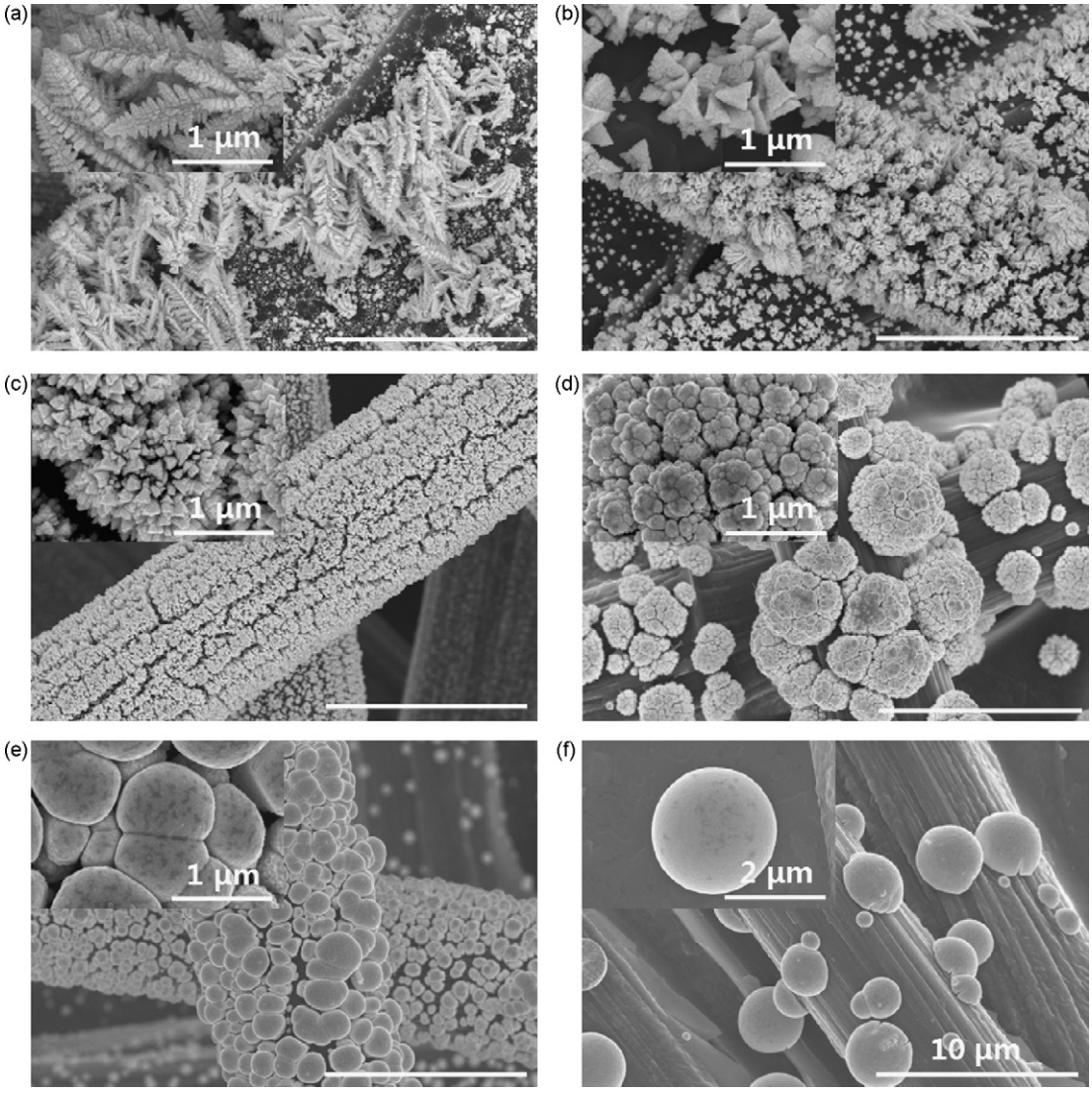

Fig. 2. SEM images of Pt on carbon paper. Electrodeposition potentials of Pt at (a) −0.2 V, (b) −0.1 V, (c) 0 V, (d) 0.1 V, (e) 0.2 V, and (f) 0.3 V (vs. Ag/AgCl) (Inset: magnified image).

posited Pt on carbon substrate shows polycrystalline structure and constant relative intensity. Therefore we could not expect structure sensitivity in our study. Average particle sizes of Pt calculated with Debye–Scherrer equation [25] with full-width at half-maximum (FWHM) values for Pt(1 1 1) and (2 0 0) are summarized in Table 1. The results of average particle size of Pt(1 1 1) and Pt(2 0 0) are ranged between 8 and 26 nm and it indicates that lower applied potential caused the increase of the crystal size in both cases of Pt(1 1 1) and Pt(2 0 0).

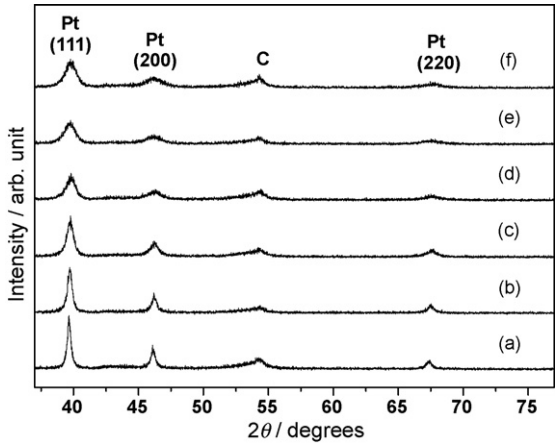

Fig. 3. XRD patterns of Pt electrodes: (a) −0.2 V, (b) −0.1 V, (c) 0 V, (d) 0.1 V, (e) 0.2 V, and (f) 0.3 V.

The particle size of Pt nanoparticles was supported by TEM analysis as shown in Fig. 4. The size of Pt nanoparticle from TEM images shows nearly the same value and tendency depending on applied potentials with XRD results. In addition, all of electrodeposited Pt particles showed polycrystalline structures by ED pattern

Table 1
FWHM and average particle sizes of Pt calculated with XRD results.

Deposition potential (V vs. Ag/AgCl)	Pt(1 1 1)		Pt(2 0 0)	
	FWHM (°)	Particle size (Å)	FWHM (°)	Particle size (Å)
0.3	0.938	90	1.110	78
0.2	0.933	91	1.113	78
0.1	0.822	103	0.875	99
0	0.587	144	0.593	146
−0.1	0.396	214	0.420	206
−0.2	0.320	264	0.384	226

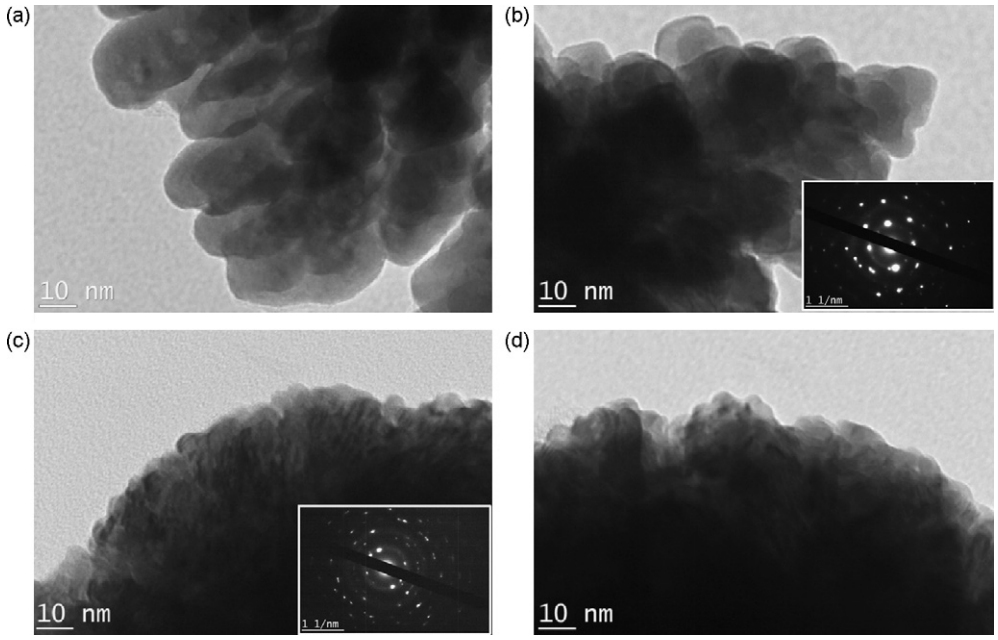

Fig. 4. TEM images of Pt electrodeposited at (a) −0.2 V, (b) 0 V, (c) 0.2 V, and (d) 0.3 V (inset: ED pattern).

analysis and the case of 0 V in Fig. 4(b) represented rather well ordered crystallinity than 0.2 V in Fig. 4(c). Considering SEM, XRD and TEM results, we can conclude that higher potential causes agglomerated morphologies with small grain boundaries of Pt, while lower potential results in dispersed morphologies with larger grain boundaries of Pt on the carbon substrate. At low deposition potentials where mass transfer is limited, an increase in separation distance between nuclei (formed on the surface of electrodeposited Pt nanoparticles) leads to dendrite structures. And at high potential where deposition kinetics are limited, smooth surfaces are favored [21].

To investigate the electrocatalytic activity of various Pt particles on carbon substrate, the cyclic voltammograms in 0.5 M $HClO_4$ solution were performed (see Fig. 5(a)). Pt deposited at 0 V (ii) exhibits the largest hydrogen and oxygen adsorption/desorption area compared to −0.2 V (i), 0.2 V (iii), and 0.3 V (iv). It means that well dispersed pyramidal Pt has the largest active surface area while the smallest one appears at hemi-spherical structure. Dotted line (v) indicates electrochemically oxidized carbon substrate. From these results, the active surface area of electrodeposited Pt is strongly associated with its morphology rather than average particle size. And commercial Pt/C was also compared with electrodeposited Pt. Pt/C has the larger active surface area and double layer capacitance in H_2SO_4 solution.

Electrodeposited Pt electrodes were applied for electrocatalytic oxidation for formic acid as illustrated in Fig. 5(b). LSV in 0.5 M $HClO_4$ solution in the presence of 0.1 M HCOOH was performed with a scan rate of 10 mV s^{-1}. The onset potential of formic acid oxidation of Pt deposited at 0 V (ii) is about −0.03 V and exhibited higher current density between 0.0 and 0.5 V. Two peaks of the oxidation of formic acid are obtained; the first anodic peak at 0.35 V is attributed to the direct oxidation of formic acid to CO_2 on the remaining sites unblocked by intermediate species, and the second peak at 0.50 V is related to the oxidation of adsorbed intermediate species of CO which releases the free surface sites for the subsequent oxidation of formic acid [17]. Pt electrodes at other deposition potentials of −0.2 (i), 0.2 (iii), and 0.3 V (iv) showed lower onset potentials than that of Pt deposited at 0 V. We understood that more active sites of Pt for adsorption of oxygen species resulted in better oxidation activity of formic acid. In spite of the largest active surface area in H_2SO_4 solution, Pt/C exhibited similar activity to electrodeposited Pt in formic acid oxidation. It means an activity for formic acid oxidation on Pt catalyst can be affected by its structures and controlling Pt morphology is effective despite having larger particle size.

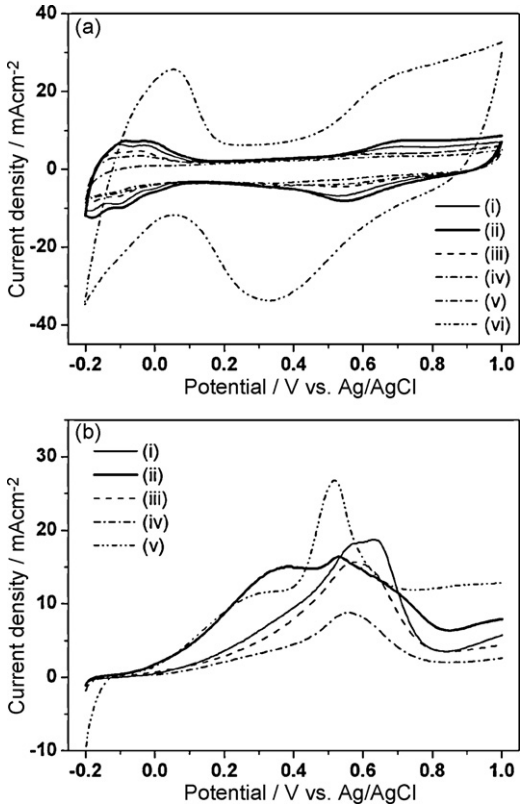

Fig. 5. Electrochemical behavior of electrodeposited Pt electrodes: (a) cyclic voltammograms (scan rate = 50 mV s^{-1}) in 0.5 M $HClO_4$, ((i) −0.2 V, (ii) 0 V, (iii) 0.2 V, (iv) 0.3 V (v) carbon fiber substrate and (vi) Pt/C), and (b) linear sweep voltammogram in 0.1 M formic acid (scan rate = 10 mV s^{-1}). Supporting electrolyte = 0.5 M $HClO_4$, ((i) −0.2 V, (ii) 0 V, (iii) 0.2 V, (iv) 0.3 V and (v) Pt/C).

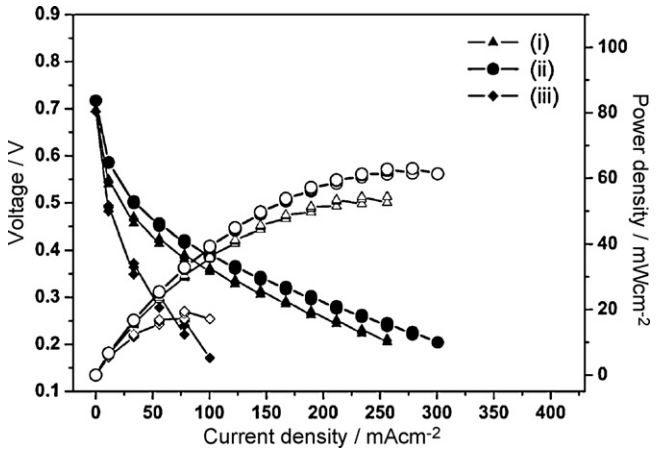

Fig. 6. Current–voltage polarization curves of electrodeposited Pt electrodes: (a) −0.2 V, (b) 0 V, (c) 0.2 V. 3 M. Formic acid = 3 mL min^{-1}, air = 200 mL min^{-1}, Cell temperature = 60 °C.

The final criterion for the preparation of electrodeposited Pt catalysts is the successful application as anode electrodes in an actual formic acid fuel cell system. For the single cell test of electrodeposited Pt electrodes, we selected representative three morphologies such as dendrite, pyramid, and hemi-sphere with operating condition of 3 M formic acid at 60 °C as shown in Fig. 6. The open circuit voltage (OCV) of Pt electrodes is about 0.7 V and the maximum power density of −0.2 V (a), 0 V (b), and 0.2 V (c) are 54, 63, and 19 mW cm^{-2}, respectively. This power density is not too low when compared to Pt-based catalysts and supported Pt catalysts. Rice et al. reported that up to 48.8 mW cm^{-2} of power densities were obtained using Pt-based catalyst at 60 °C with O_2 supply [26]. And Liu et al. prepared carbon-supported Pt catalysts which exhibited 116 mW cm^{-2} at 50 °C with 8 mg cm^{-2} of anode catalyst and O_2 supply [27]. Considering low catalyst loading of 0.5 mg cm^{-2} and air supply used in our study, electrochemically deposited Pt catalysts shows relatively good performance for fuel cell application. Moreover, the tendency of single cell performance of electrodeposited Pt is similar to the results of half cell observations in Fig. 5 and we conclude that the morphology of Pt could influence on the performance of DFAFC.

4. Conclusions

Dendritic, pyramidal, cauliflower-like, and hemi-spherical morphologies of Pt governed by applied potentials from −0.2 to 0.3 V (vs. Ag/AgCl) are electrodeposited on carbon paper. As the overpotential increases to the limiting current, dendritic bulky particles over 20 nm are formed. Low overpotential, however, causes dense hemi-spherical structure less than 10 nm. Controlled morphologies of Pt are applied for an electrocatalytic oxidation of formic acid and well dispersed pyramidal Pt morphology of 0 V with ca. 14 nm particle size represents the highest activity in both half and single fuel cell measurements. Homogeneous distribution of pyramidal structure of Pt on carbon paper leading to a high surface to volume ratio is the reason of the highest activity for formic acid oxidation.

Acknowledgements

This work was supported by New & Renewable Energy R&D program(20093020030020-11-1-000) under the Ministry of Knowledge Economy, Republic of Korea.

References

[1] S. Ha, R. Larsen, Y. Zhu, R.I. Masel, Fuel Cells 4 (2004) 337–343.
[2] C.M. Miesse, W.S. Jung, K.-J. Jeong, J.K. Lee, J. Lee, J. Han, S.P. Yoon, S.-W. Nam, T.-H. Lim, S.-A. Hong, J. Power Sources 162 (2006) 532–540.
[3] S. Kang, J. Lee, J.K. Lee, S.-Y. Chung, Y. Tak, J. Phys. Chem. B 110 (2006) 7270–7274.
[4] Y.X. Chen, M. Heinen, Z. Jusys, R.J. Behm, Angew. Chem. Int. Ed. 45 (2006) 981–985.
[5] S.E. Habas, H. Lee, V. Radmilovic, G.A. Somorjai, P. Yang, Nat. Mater. 6 (2007) 692–697.
[6] S. Uhm, H.J. Lee, Y. Kwon, J. Lee, Angew. Chem. Int. Ed. 47 (2008) 10163–10166.
[7] J. Chen, B. Lim, E.P. Lee, Y. Xia, Nano Today 4 (2009) 81–95.
[8] B. Wiley, Y.G. Sun, B. Mayers, Y.N. Xia, Chem. Eur. J. 11 (2005) 454–463.
[9] J.Y. Chen, T. Herricks, Y.N. Xia, Angew. Chem. Int. Ed. 44 (2005) 2589–2592.
[10] F. Kim, S. Connor, H. Song, T. Kuykendall, P.D. Yang, Angew. Chem. Int. Ed. 43 (2004) 3673–3677.
[11] V.F. Puntes, K.M. Krishnan, A.P. Alivisatos, Science 291 (2001) 2115–2117.
[12] R.C. Jin, Y.W. Cao, C.A. Mirkin, K.L. Kelly, G.C. Schatz, J.G. Zheng, Science 294 (2001) 1901–1903.
[13] L. Tian, Y. Qi, B. Wang, J. Colloid Interface Sci. 333 (2009) 249–253.
[14] J.W. Dini, Plat. Surf. Finish. 75 (1988) 11.
[15] R.S. Jayashree, J.S. Spendelow, J. Yeom, C. Rastogi, M.A. Shannon, P.J.A. Kenis, Electrochim. Acta 50 (2005) 4674–4682.
[16] S. Uhm, S.T. Chung, J. Lee, Electrochem. Commun. 9 (2007) 2027–2031.
[17] J.K. Lee, H. Jeon, S. Uhm, J. Lee, Electrochim. Acta 53 (2008) 6089–6092.
[18] A.C. Hill, R.E. Patterson, J.P. Sefton, M.R. Columbia, Langmuir 15 (1999) 4005–4010.
[19] S. Uhm, Y. Kwon, S.T. Chung, J. Lee, Electrochim. Acta 53 (2008) 5162–5168.
[20] S. Uhm, T. Noh, Y.D. Kim, J. Lee, ChemPhysChem 9 (2008) 1425–1429.
[21] L.M. Plyasova, I.Y. Molina, A.N. Gavrilov, S.V. Cherepanova, O.V. Cherstiouk, N.A. Rudina, E.R. Savinova, G.A. Tsirlina, Electrochim. Acta 51 (2006) 4477–4488.
[22] J. Clavilier, R. Parsons, R. Durand, C. Lamy, J.M. Leger, J. Electroanal. Chem. 124 (1981) 321–326.
[23] C. Lamy, J.M. Leger, J. Clavilier, R. Parsons, J. Electroanal. Chem. 150 (1983) 71–77.
[24] R.R. Adzic, A.V. Tripkovic, W. O'Grady, Nature 296 (1982) 137–138.
[25] A.L. Patterson, Phys. Rev. 56 (1939) 972–977.
[26] C. Rice, R.I. Ha, R.I. Masel, P. Waszczuk, A. Wieckowski, T. Barnard, J. Power Sources 111 (2002) 83–89.
[27] Z. Liu, L. Hong, M.P. Tham, T.H. Lim, H. Jiang, J. Power Sources 161 (2006) 831–835.